Silurian strontium isotope stratigraphy

Karem Azmy* *Ottawa-Carleton Geoscience Centre, University of Ottawa, Ottawa, Ontario K1N 6N5, Canada*

Jan Veizer *Ottawa-Carleton Geoscience Centre, University of Ottawa, Ottawa, Ontario K1N 6N5, Canada,* and *Institut für Geologie, Ruhr Universität, 44780 Bochum, Germany*

Bernd Wenzel *Institut für Geologie der Universität Erlangen-Nürnberg, 91054 Erlangen, Germany*

Michael G. Bassett *Department of Geology, National Museum of Wales, Cardiff CF1 3NP, United Kingdom*

Paul Copper *Department of Earth Sciences, Laurentian University, Sudbury, Ontario P3E 2C6, Canada*

ABSTRACT

A sample set of 164 calcitic brachiopod shells, covering the entire Silurian Period (~ 30 m.y.) with a resolution of about 0.7 m.y., was collected from stratotype sections at Anticosti Island (Canada), Wales (United Kingdom), Gotland (Sweden), Podolia (Ukraine), Latvia, and Lithuania. They show $^{87}Sr/^{86}Sr$ values ranging from 0.707930 to 0.708792 that progressively increase with time. This may indicate an increasing riverine flux of radiogenic Sr into the ocean from weathering of continental sialic rocks due to progressive warming of the climate. Exceptionally high increases in $^{87}Sr/^{86}Sr$ values were observed in early Llandovery (Rhuddanian), late Llandovery (Telychian), and late Ludlow (Gorstian-Ludfordian boundary) samples. Partial linear regressions, based on a stepwise climbing pattern, with local drops around the Llandovery-Wenlock boundary and in latest Ludlow time, were used to estimate relative ages with a resolution of about ±2 biozones (~1.5–2 m.y.). The Sr-isotope curve shows distinct inflection points in earliest Wenlock and mid-Přídolí time. These may be used to correlate the Llandovery-Wenlock boundary in the United Kingdom, Gotland, and Lithuania, and the Kaugatuma-Ohesaare boundary in the Baltic states and Podolia.

INTRODUCTION

Variations in seawater $^{87}Sr/^{86}Sr$ over geologic time, particularly for Phanerozoic time, have been used to reconstruct the evolutionary history of ancient seawater (e.g., Veizer and Compston, 1974; Burke et al., 1982; Veizer, 1989; McArthur, 1994), to understand continental weathering processes and mid-oceanic ridge hydrothermal circulation (cf. Hodell et al., 1990; Richter et al., 1992; Farrell et al., 1995), and to correlate and date marine sedimentary rocks (e.g., Elderfield, 1986; Quinn et al., 1991; McArthur, 1994). The dominant driving forces causing the changes in seawater isotopic ratios are suggested to be (1) continental runoff and ground-water runout, both of which supply radiogenic strontium to the oceans, and (2) seawater–oceanic crust interaction, particularly hydrothermal rift–related activities, supplying a less-radiogenic strontium (Palmer and Elderfield, 1985). Other factors, such as diagenetic flux and carbonate recycling, may account for a minor contribution (Elderfield, 1986; Veizer, 1989).

Low-Mg calcite brachiopod shells, particularly if nonluminescent, have been documented to frequently retain the primary Sr-isotope signals of ambient seawater (Popp et al., 1986; Banner and Kaufman, 1994; Diener et al., 1996). When biogenic marine carbonate forms, the $^{87}Sr/^{86}Sr$ of ocean water is incorporated into its structure without fractionation. Oceanic uniformity of $^{87}Sr/^{86}Sr$ at any given time is expected, because the residence time of Sr in the oceans (~ 10^6 yr) is much longer than the time it takes for currents to mix the oceans (Faure, 1986). However, for highly stratified oceans, the response may be different due to possible mixing rates of bottom waters approaching the residence times for Sr in seawater (McArthur, 1994).

Variations in $^{87}Sr/^{86}Sr$ composition of past seawater, resolvable on a short-time scale of 10^7 to 10^6 yr, may be utilized for high-resolution stratigraphic correlations with an accuracy comparable to, and perhaps higher than, that of biostratigraphy, the latter usually being 1 to 5 m.y. The condition is that the temporal $^{87}Sr/^{86}Sr$ trends are characterized by steep slopes. This was the case for several intervals of Phanerozoic time, and particularly in Cenozoic time (e.g., Mead and Hodell, 1995).

The main objectives of this study are to (1) refine the Sr-isotope curve for the Silurian seawater, (2) utilize such a refined curve for high-resolution stratigraphic correlation, and (3) improve understanding of geochemical cycling for Sr during Silurian time.

GEOLOGICAL SETTING

The samples for this study were selected from diverse depositional settings on different paleocontinents. Paleogeographic reconstructions (cf. McKerrow et al., 1991) place all these basins within the tropical paleolatitudes and they include Anticosti Island, Québec, Canada (Laurentia), England, Sweden, Lithuania, Latvia, and Podolia in the Ukraine (Baltica). The lithology of the studied sequences comprised mainly limestones of shallow shelf environments, frequently associated with reefs. The stratigraphic assignment of these sections (Fig. 1) follows the global Silurian standard time scale. For further details of geology and samples see Azmy (1996), Azmy et al. (1998), Wenzel and Joachimski (1996), and Wenzel (1997).

METHODOLOGY

The selected brachiopods were identified and two identical slabs (~1.5 mm thick) were cut longitudinally through the umbo zone, using an ISOMET low-speed saw. The slabs were gently polished on a glass plate using Al_2O_3 powder (size 9.5 µm). A thin section of the sample, made

*E-mail: azmy@science.uottawa.ca.

Data Repository item 9933 contains additional material related to this article.

GSA Bulletin; April 1999; v. 111; no. 4; p. 475–483; 7 figures; 3 tables.

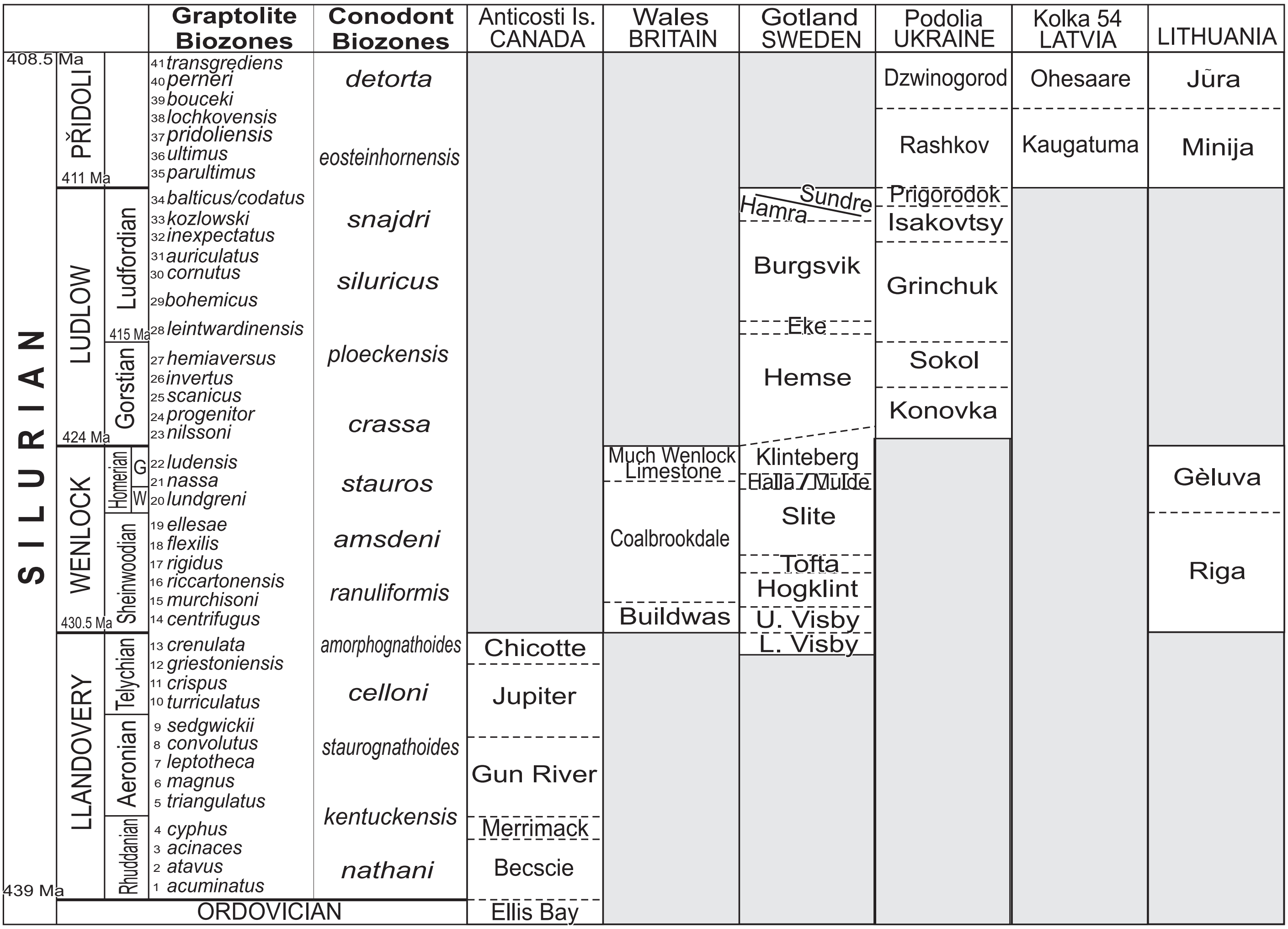

Figure 1. Sampled Silurian sections and their stratigraphic assignments (modified from Basset et al., 1989; Siveter et al., 1989; Jin et al., 1990; Kaminskas and Musteikis, 1994; Long and Copper, 1994).

from one of the slabs, was studied under a polarizing microscope to examine the preservation of the calcite fibers. The thin section and the other polished slab were viewed under cathodoluminescence, with the operating conditions at ~10 to 11 kv, gun current of 350 to 400 mA, and vacuum of ~ 0.03 Torr.

Carbonate material from the nonluminescent parts of the secondary layer was microsampled from the slab under a binocular microscope by smashing the shell with a stainless steel dental pick. The fragments were cleaned in an ultrasonic bath.

A fragment from each sample was studied under a scanning electron microscope to examine the preservation of the calcite crystals. The rest of the sample was ground in an acid-washed agate mortar and ~ 3 mg were used for trace element analysis by a Thermo Jarrell Ash-AtomScan 25 inductively coupled plasma source spectrometer, at the University of Ottawa, to test for shell chemical preservation (Azmy, 1996).

For Sr-isotope analysis, about 1 mg of the powdered sample was dissolved for 30 min in 1.5 ml of 2.5N suprapure HCl at room temperature, and Sr was extracted via a clean 10 ml column filled with Dowex AG50-X8 cation resin. The eluent was dried at 125 °C for 2 hr. The dried sample was dissolved in 0.01N HCl for a few minutes and passed through a clean 10 ml separation column filled with Teflon resin to trap Ca that may not have been separated from Sr by first column. The collected sample was evaporated at 125 °C for 2 hr to be ready for running on the mass spectrometer. Blank samples were frequently run and spiked using ^{84}Sr to measure any contamination that might occur during the process of separation.

The sample was dissolved in 0.4 ml of 1M H_3PO_4 for 2 min and about half of it was loaded on a tantalum filament. The strontium isotope ratio was measured using the Finnigan MAT 261 multicollector thermal ionization mass spectrometer at Carleton University. The laboratory standard used was NBS 987 (^{87}Sr/^{86}Sr = 0.710249) with a (2σ) precision calculated from 30 measurements of ± 0.000017. The blanks were 0.4 to 0.8 ng. The measured Sr isotope data are listed in Table DR1, GSA Data Repository.[1] For further details of geology, samples, and analytical and selection procedures, see Azmy (1996) and Azmy et al. (1998).

Another set of brachiopod samples, from Gotland, was prepared and measured independently at the laboratory of Ruhr Universität in Bochum fol-

[1]GSA Data Repository item 9933, Table DR1, is available on request from Documents Secretary, GSA, P.O. Box 9140, Boulder, CO 80301. E-mail: editing@geosociety.org. Web: http://www.geosociety.org/pubs/ftpyrs.htm.

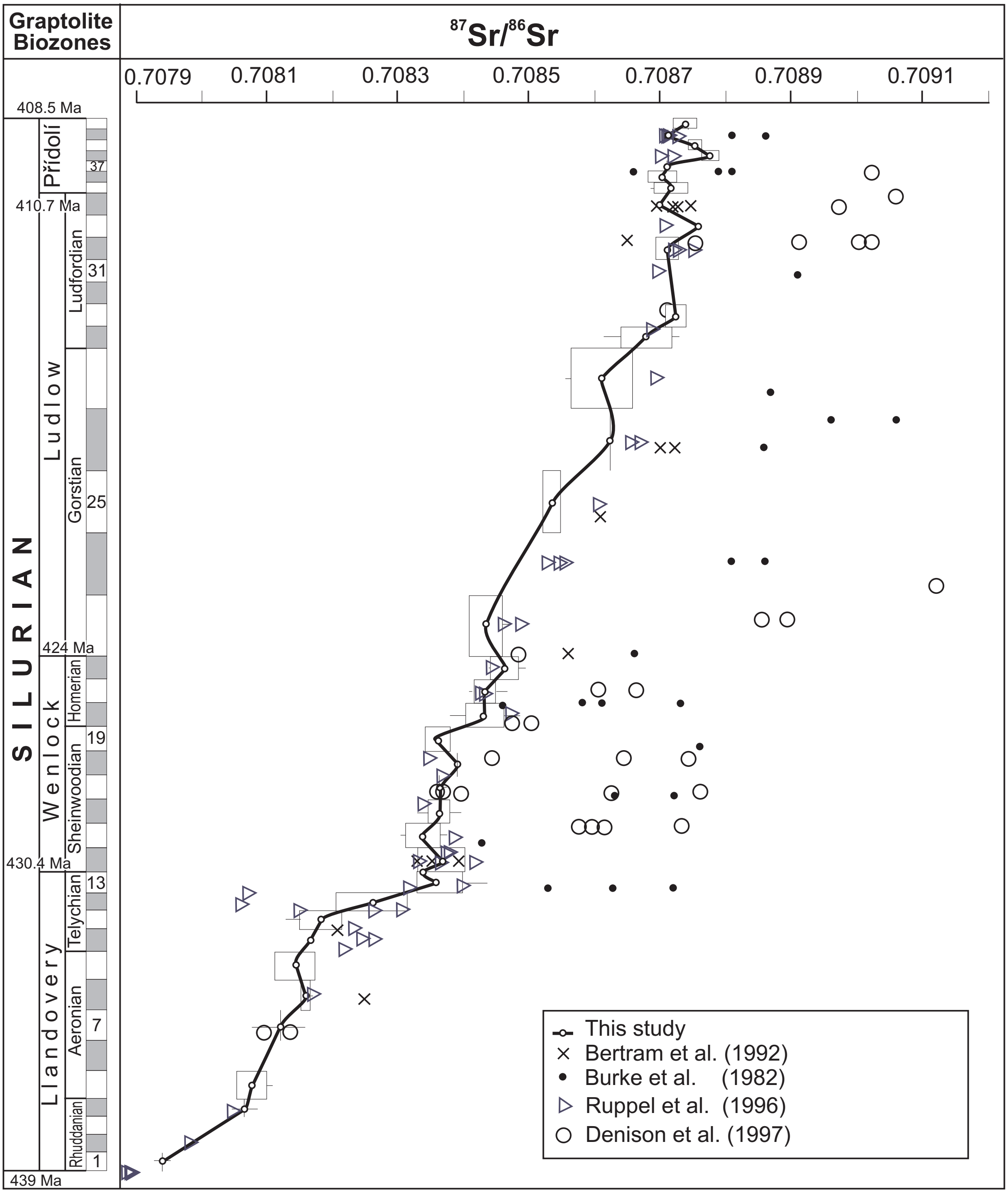

Figure 2. The evolution of ^{87}Sr/^{86}Sr ratios throughout the Silurian Period based on this study, with comparison to published results of Burke et al. (1982), Bertram et al. (1992), Ruppel et al. (1996), and Denison et al. (1997). Boxes and bars refer to ± 1σ (standard deviations) and to the ranges of data for single biozone, respectively. Biozonation (1 to 41) and numerical ages are as in Figure 1. All available ^{87}Sr/^{86}Sr data were normalized to 0.710249 for the NBS 987 standard. There is a spread of data within a single biozone despite the high quality of the database (see Fig. 4). Since the biozone is the smallest correlatable unit, the observed spread could be resolved into temporal succession only if all good samples could have been collected from the same complete section, a requirement generally beyond geological reality. This is the reason for boxes.

lowing the procedure of Diener et al. (1996). Only splinters from nonluminescent shells that exhibited well-preserved fibrous microstructure were picked. A sample of 0.5 to 2 mg was dissolved in 2.5 N suprapure HCl and, after evaporation, Sr was extracted with quartz glass exchange columns filled with Bio Rad AG50Wx8 ion-exchange resin. Then, 150–250 ng Sr were loaded on Re filaments using a Ta_2O_5–HNO_3–HF–H_3PO_4 solution. Measurements were performed with a Finnigan MAT 262 multicollector mass spectrometer. The NBS 987 value was 0.710244 ± 0.000008. The measured isotope data are highlighted in Table DR1 (see footnote 1). For further details of geology, samples, and analytical and selection procedures, see Wenzel (1997). (All data shown in figures in this paper are normalized to the NBS 987 standard, 0.710249.)

PREVIOUS WORK

The temporal oscillations in the Sr isotopic composition of the Phanerozoic seawater were outlined by Burke et al. (1982), but their work was based mostly on whole-rock samples (e.g., Denison et al., 1997). Due to possible distortion of the original $^{87}Sr/^{86}Sr$ signal by diagenetic alteration, other materials have been suggested for development of a seawater curve, including evaporitic minerals, biogenic carbonates, marine barite, apatite (conodonts, fish teeth, and bones), and marine carbonate cements (Burke et al., 1982; Popp et al., 1986; Banner and Kaufman, 1994; Bertram et al., 1992; Ruppel et al., 1996; Montanez et al., 1996; Denison et al., 1997). Among these more refined studies, only Bertram et al. (1992) and Ruppel et al. (1996) provided data for the Silurian Period, based on phosphatic fossil conodonts. These data have less scatter and also are closer to the lower limit of the Burke et al. (1982) trend; Ruppel et al. (1996) measurements generally have the least radiogenic values (Fig. 2). The observed scatter in the published data may be attributed to either partial diagenetic alteration of the analyzed samples or to uncer-

TABLE 1. MEAN, STANDARD DEVIATION, MAXIMUM, AND MINIMUM Sr-ISOTOPE VALUES CALCULATED FOR EACH GRAPTOLITE BIOZONE IN THE BIOCORRELATION OF SILURIAN PERIOD

Biozone	Age (Ma)	n	$^{87}Sr/^{86}Sr_{mean} \pm 1\sigma$	Maximum	Minimum
41 *transgrediens*	408.7	2	0.708740 ± 0.000017	0.70875	0.70873
40 *permeri*	409.0	2	0.708715 ± 0.000008	0.70872	0.70871
39 *bouceki*	409.3	1	0.708755		
38 *lochkovensis*	409.6	3	0.708779 ± 0.000012	0.70879	0.70877
37 *pridoliensis*	409.9	1	0.708713		
36 *ultimus*	410.2	4	0.708706 ± 0.000021	0.70873	0.70868
35 *parultimus*	410.5	4	0.708719 ± 0.000025	0.70874	0.70869
34 *balticus*	411.0	5	0.708762 ± 0.000005	0.70871	0.7087
33 *kozlowskii*	411.6	2	0.708759 ± 0.000003	0.70876	0.70876
32 *inexpectatus*	412.3	2	0.708713 ± 0.000006	0.70872	0.70875
29 *bohemicus*	414.2	4	0.708726 ± 0.000015	0.70874	0.70871
28 *leintwardinensis*	414.8	9	0.708681 ± 0.000038	0.70873	0.70862
27 *hemiaversus*	416.0	5	0.708613 ± 0.000046	0.70865	0.70856
26 *invertus*	417.8	1	0.708625		
25 *scanicus*	419.6	4	0.708537 ± 0.000013	0.70855	0.70852
23 *nilssoni*	423.1	4	0.708436 ± 0.000025	0.70847	0.70842
22 *ludensis*	424.4	8	0.708464 ± 0.000020	0.7085	0.70844
21 *nassa*	425.1	17	0.708434 ± 0.000015	0.70847	0.70841
20 *lundgreni*	425.8	10	0.708440 ± 0.000028	0.70849	0.70838
19 *ellesae*	426.5	6	0.708362 ± 0.000018	0.70838	0.70834
18 *flexilis*	427.2	1	0.708393		
17 *rigidus*	427.9	3	0.708369 ± 0.000136	0.70837	0.70837
16 *riccartonensis*	428.6	16	0.708364 ± 0.000015	0.7084	0.70833
15 *murchisoni*	429.3	6	0.708379 ± 0.000026	0.70838	0.70831
14 *centrifugus*	430.0	2	0.708367 ± 0.000035	0.70839	0.70834
13 *crenulata* / 14 *centrifugus*	430.4	2	0.708339 ± 0.000000	0.708339	0.70834
13 *crenulata*	430.7	9	0.708366 ± 0.000034	0.70844	0.70834
12 *griestoniensis*	431.2	4	0.708261 ± 0.000054	0.70832	0.70821
11 *crispus*	431.7	5	0.708182 ± 0.000031	0.70821	0.70813
10 *turriculatus*	432.3	1	0.708167		
9 *sedgwickii*	433.0	3	0.708143 ± 0.000031	0.70818	0.70812
8 *convolutus*	433.9	5	0.708159 ± 0.000008	0.70817	0.70815
7 *leptotheca*	434.8	2	0.708120 ± 0.000016	0.70816	0.70808
5 *triangulatus*	436.5	6	0.708077 ± 0.000022	0.70811	0.70805
4 *cyphus*	437.2	2	0.708065 ± 0.000021	0.70808	0.70805
1 *acuminatus*	438.7	2	0.707941 ± 0.000015	0.70795	0.70793

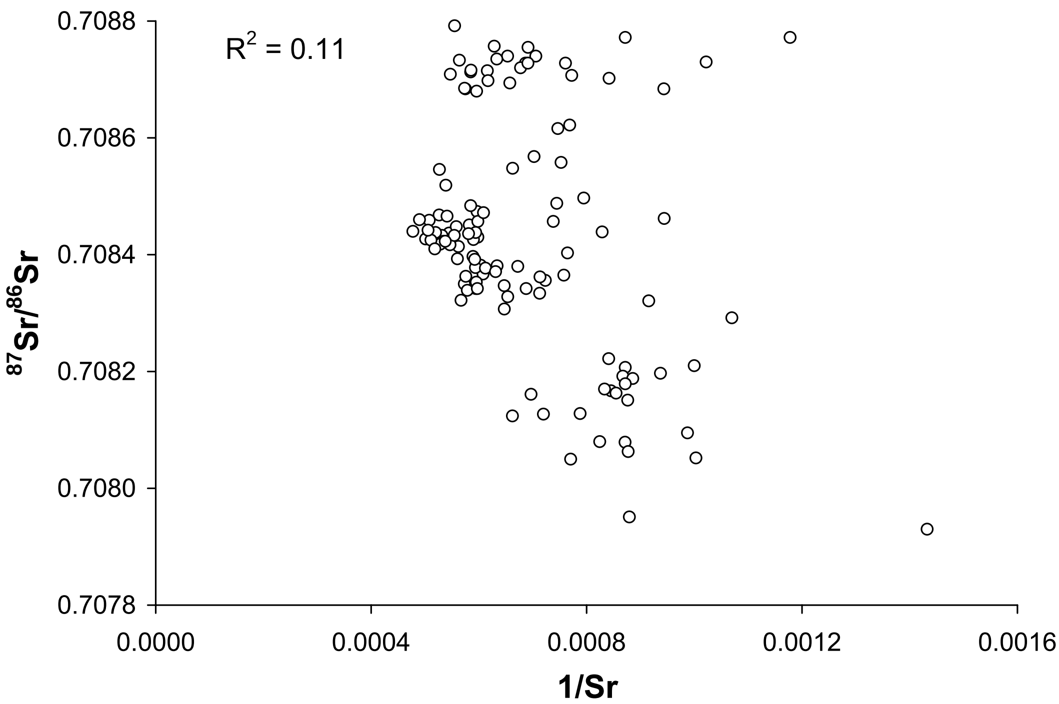

Figure 3. Scatter diagram of 1/Sr vs. $^{87}Sr/^{86}Sr$ for the Silurian brachiopods.

TABLE 2. THE ERROR IN AGE CALCULATED FOR EACH SEGMENT OF THE SILURIAN REGRESSION PLOT BASED ON CONFIDENCE INTERVAL AT THE 95% LEVEL

Segment	Error (in Ma)	Error (in biozones)	Covered epoch
VI	±2.1 to 2.2	5	Přídolí
V	±0.8 to 0.9	2	Late Ludlow
IV	±2.1 to 2.5	2	Ludlow
IV	±2.1 to 2.5	4	Wenlock
III	±0.9 to 1.0	2	Late Llandovery
II	±2.3 to 2.5	3	Mid-Llandovery
I	±1.1 to 1.2	2	Early Llandovery

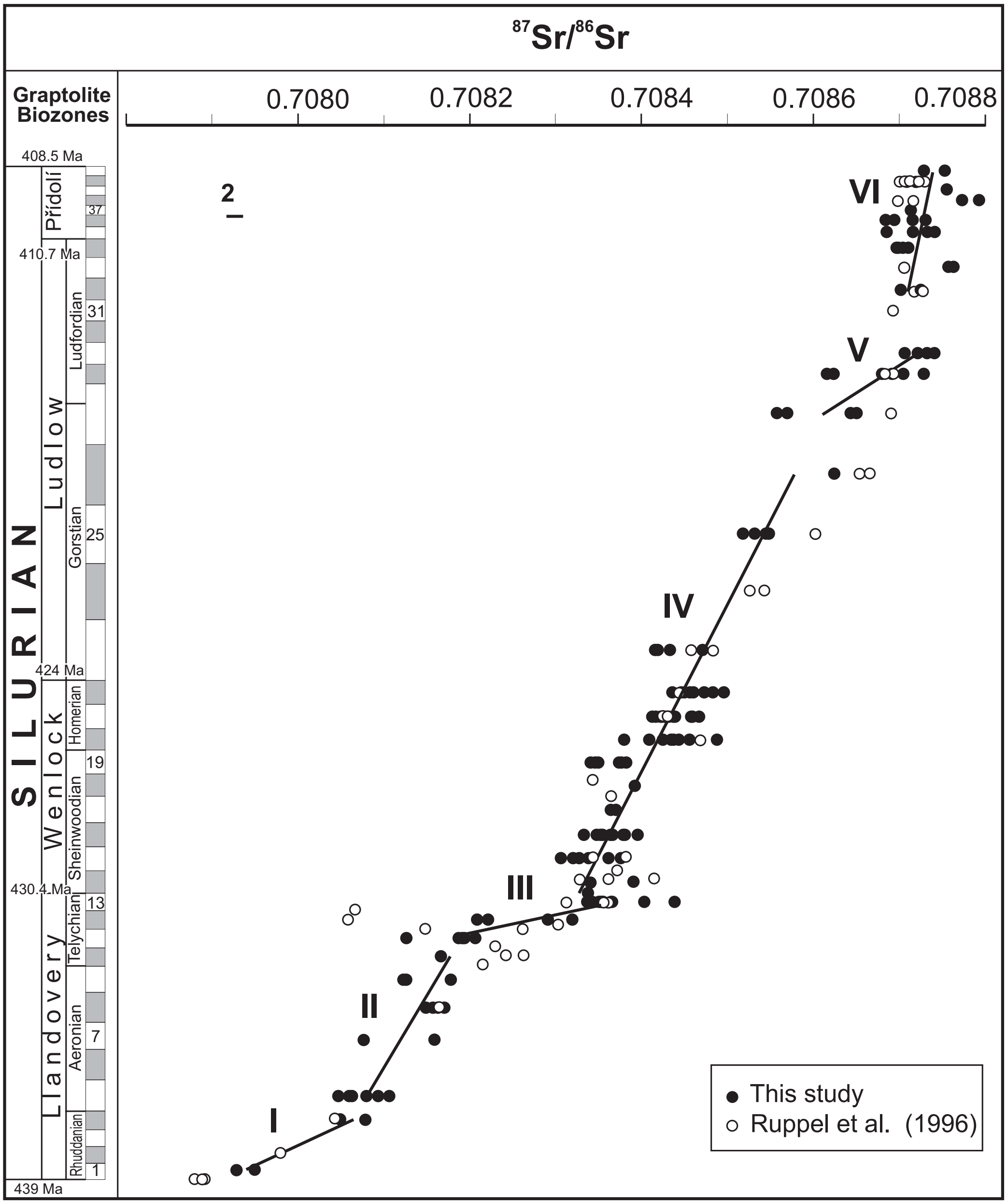

Figure 4. The Silurian $^{87}Sr/^{86}Sr$ values vs. age. Heavy lines are the best-fit regression lines. Biozonation and numerical ages were generated using the same parameters as in Figures 1 and 2. The 2σ bar in the upper left corner refers to an error bar typical for a single point. In the conodont set of Ruppel et al. (1996), 30 measurements (including 9 duplicates) are considerably offset from our brachiopod data. Only 32 of their close samples are, therefore, utilized as a stratigraphic test set (see Table 3).

tainties in their age assignment. The incorporated impurities may also contribute to the distortion of the $^{87}Sr/^{86}Sr$ values. Ruppel et al. (1996) reported some cyclic trends on the 10^6 yr time scale, but the amplitudes of these oscillations (0.000015) are within the documented $^{87}Sr/^{86}Sr$ intraspecimen variations for conodonts. The published Silurian data reveal a general trend of increasing $^{87}Sr/^{86}Sr$ values with time (Fig. 2).

SILURIAN STRONTIUM-ISOTOPE CURVE BASED ON BRACHIOPODS

The current Sr-isotope curve for the Silurian Period (Fig. 2 and Table 1) covers the entire period, estimated to have lasted about 30 m.y., from 439 ± 7 to 408.5 ± 4 Ma (Harland et al., 1990). This time span includes 41 graptolite biozones (Figs. 1and 2), each with an estimated duration of less than 1 m.y., except for Gorstian time (early Ludlow), which includes biozones lasting to 2 m.y. The shape of the curve is mainly controlled by (1) accuracy of the relative age model used to calibrate the isotope curve, (2) temporal variations in the $^{87}Sr/^{86}Sr$ value of Silurian seawater, (3) postdepositional alteration of brachiopod shells, and (4) analytical errors (cf. McArthur, 1994).

Postdepositional alteration was discussed in detail in Azmy (1996), Azmy et al. (1998), Wenzel and Joachimski (1996), and Wenzel (1997), with the conclusion that petrographic (cathodoluminescence and SEM) and chemical properties of the studied shells all demonstrated an outstanding degree of preservation of the shell ultrastructure. The relatively low variability of Sr concentrations and the weak correlation between Sr content and $^{87}Sr/^{86}Sr$ (Fig. 3) are also consistent with such an interpretation and the measurements probably reflect the range of original values. Analytical errors account for only about 0.000015 of the signal (cf. McArthur, 1994) and thus are probably negligible. As a result, the data based on brachiopods have less scatter and are typically less radiogenic than the published data from coeval whole rocks (Burke et al., 1982; Denison et al., 1997) and phosphatic conodonts (Bertram et al., 1992; Ruppel et al., 1996). The present scatter for the majority of biozones is small, with a 2σ range of less than 0.00003 (Fig. 2).

Taking into account these clarifications, the band is considered to reflect mainly temporal changes in Sr-isotopic composition of Silurian seawater, with the proviso that the assigned numerical ages depend on extrapolation from graptolite zones.

Although most of the previously published data are more radiogenic than the present brachiopod values, two conodont measurements of Ruppel et al. (1996) and one of Bertram et al. (1992) plot below the brachiopod trend (Fig. 2).

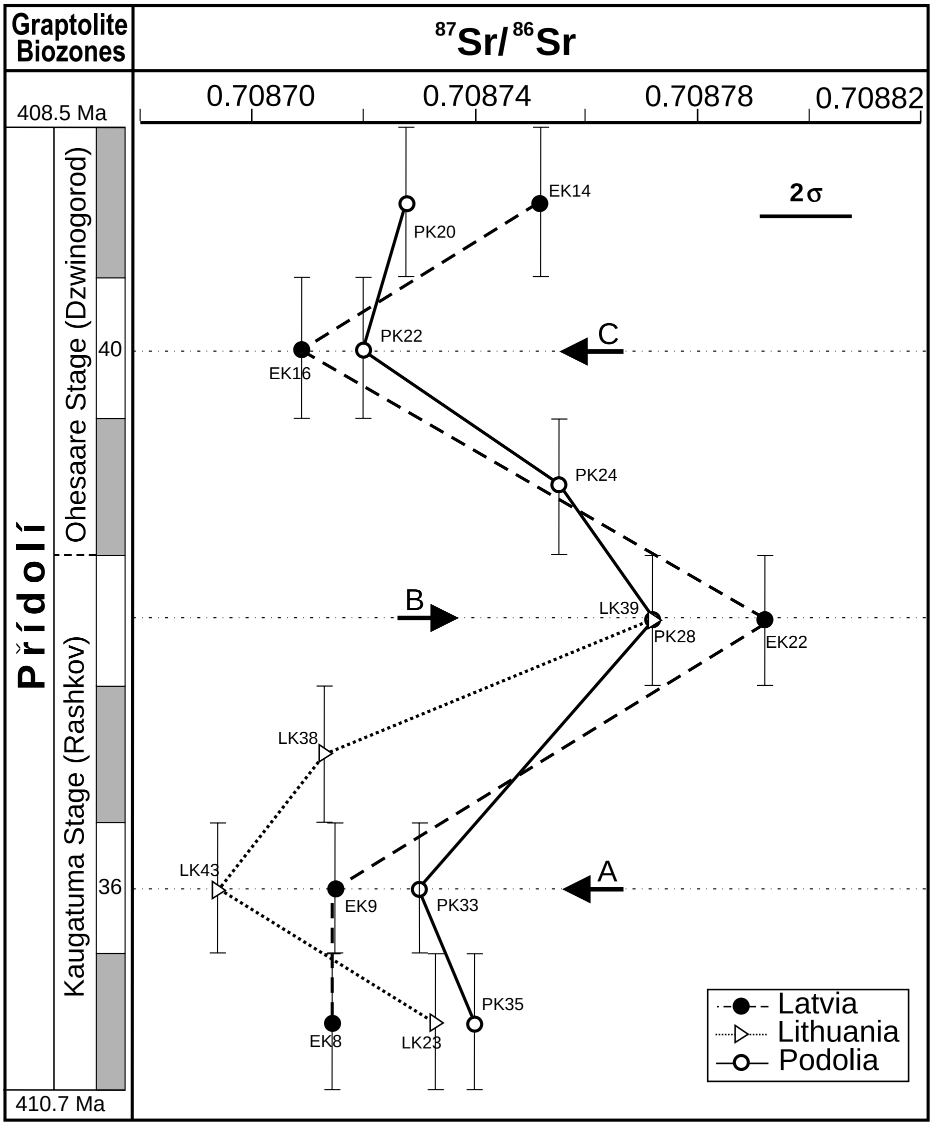

Figure 5. The inflection points (A, B, and C) revealed by comparison of $^{87}Sr/^{86}Sr$ curves of Přídolí for Latvia, Lithuania, and Podolia. Error bars for $^{87}Sr/^{86}Sr$ refer to ± 1σ values. The error bars for age are based on estimated duration of the biozones. Biozonation and numerical ages were generated using the same parameters as in Figures 1 and 2.

The reasons for this discrepancy are not clear, but an explanation may be based on a correlation mismatch (Fig. 2).

Variations in the Sr-isotope composition of seawater are mainly a function of balance between inputs of radiogenic $^{87}Sr/^{86}Sr$ from sialic continental crust and low $^{87}Sr/^{86}Sr$ from hydrothermal sources. During Silurian time, the hydrothermal input is assumed to have been less effective than the continental input due to relatively dormant volcanic activity. The progressive $^{87}Sr/^{86}Sr$ increase in Silurian seawater (Fig. 2) is easier to explain by enhanced mechanical and chemical weathering due to progressive warming of the climate (cf. McKerrow et al., 1991).

STRONTIUM-ISOTOPE STRATIGRAPHY

High-resolution strontium-isotope stratigraphy is a potential tool for correlation and dating of marine samples (cf. Hodell, 1994; McArthur, 1994). For this task, the trend of $^{87}Sr/^{86}Sr$ variations can be approximated by regressions that are either linear (e.g., Hodell et al., 1989, 1990; Oslick et al., 1994; Mead and Hodell, 1995) or curvilinear (Miller et al., 1991; Hodell and

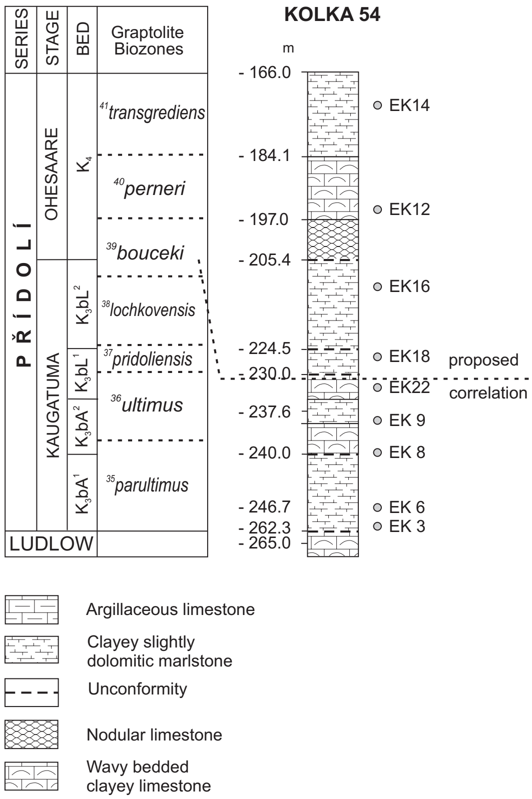

Figure 6. Stratigraphic subdivisions of Přídolí in Latvia (core Kolka 54) showing the relative position of samples (from D. Kaljo,1994, personal commun.)

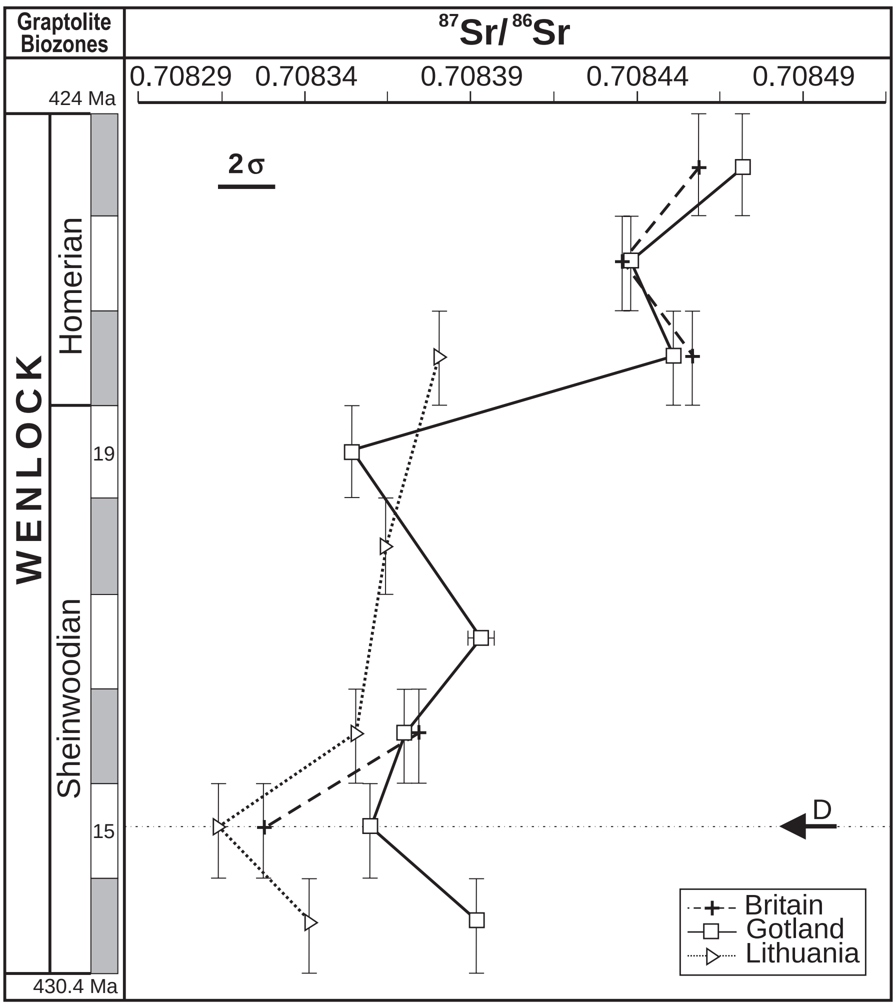

Figure 7. The inflection point (D, indicated by arrow) revealed by comparison of $^{87}Sr/^{86}Sr$ curves for the Wenlock of Wales (United Kingdom), Gotland, and Lithuania. Error bars as in Figure 6. The biozonation bar and numerical ages were generated using the same parameters as in Figures 1 and 2.

Woodruff, 1994; Oslick et al., 1994). For the current data set, modeling by simple linear regressions for specific time segments fits the $^{87}Sr/^{86}Sr$ data well (Fig. 4). The Silurian data set contains six regression segments (Table 2). The regression lines I, III, and V, of Rhuddanian (*acuminatus* to *cyphus* biozones), Telychian (*crispus* to *crenulata* biozones), and early Ludfordian (*bohemicus* to *auriculatus* biozones) ages, have significantly steeper slopes and higher R^2 values (> 0.7) than the other three segments. These steep lines may provide temporal resolution of 1 m.y. or better. Such a steep slope may reflect slow rates of sedimentation, a condensed sedimentary record, or a stratigraphic hiatus.

The regression lines depict a general stepwise climb of $^{87}Sr/^{86}Sr$ values with decreasing age, but local drops appear to exist at the commencements of segments IV and VI, the Llandovery-Wenlock boundary and latest Ludlow times, respectively (Fig. 4). The earlier drop coincides with Barrandian (Rheic) volcanism during latest Llandovery time and the latter may correlate with late Ludlow volcanic activity documented in Poland (cf. Neuman and Kershaw, 1991).

Except for the high slope segments, the regression lines are almost parallel, at a similar gentle slope (Fig. 4), suggesting a uniformly increasing rate of input of radiogenic Sr, presumably reflecting a similar increase in the riverine runoff. The generally low scatter of data points for segments I to V provides reliable age estimates. In contrast, the youngest segment, VI, of Ludfordian (late Ludlow) to Přídolí age, has a large scatter and is therefore of doubtful value for chemostratigraphy. This high scatter of data may be due to errors in correlation of biozones, to postdepositional overprinting of $^{87}Sr/^{86}Sr$ values, to nonuniform rate of sedimentation, or to a combination of all of these. It is also possible that there are short-term oscillations in the Sr isotopic composition of seawater.

The regression lines can be utilized to estimate the ages for the studied graptolite biozones. The uncertainty for the estimated ages is controlled by the degree of scatter of the data points around the regression lines, and by the slope. However, the largest uncertainty for the absolute (numerical) estimate of the age is due to the large error associated with the calibration tie points. For this reason, numerical values should be viewed only as relative superposition of biozones. In that case, the $^{87}Sr/^{86}Sr$ values can be utilized as a correlation tool, but with differing 95% confidence levels (Table 2). Excluding segment VI, where the scatter of data is high, the error in estimated ages is equivalent to about ± 2 biozones, but can be as high as ± 4 biozones in the lower part of the segment IV (Wenlock); the latter is characterized by more scattered data (Fig. 4).

TABLE 3. TEST SET FROM RUPPEL ET AL. (1996)

Sample I.D.	$^{87}Sr/^{86}Sr \pm 2\sigma$	Known age	Estimated age	Error (in biozones)
77-34A	0.708705 ± 0.000010	^{33}*kozlowskii*	^{33}*kozlowskii*	None
Hickory Ck-13	0.708726 ± 0.000013	^{32}*inexpectatus*	^{33}*kozlowskii*	1
Juves 3	0.708718 ± 0.000011	^{32}*inexpectatus*	^{33}*kozlowskii*	1
77-27	0.708725 ± 0.000009	^{32}*inexpectatus*	^{35}*parultimus*	3
77-310	0.708693 ± 0.000010	^{31}*auriculatus*	^{31}*auriculatus*	None
77-307	0.708683 ± 0.000011	^{28}*leintwardinensis*	^{28}*leintwardinensis*	None
77-25	0.708692 ± 0.000008	^{28}*leintwardinensis*	^{28}*leintwardinensis*	None
England 4.8	0.708690 ± 0.000010	^{27}*hemiaversus*	^{28}*leintwardinensis*	1
77-305	0.708665 ± 0.000011	^{26}*invertus*	^{28}*leintwardinensis*	2
77-304	0.708653 ± 0.000012	^{26}*invertus*	^{27}*hemiaversus*	1
77-303	0.708602 ± 0.000015	^{25}*scanicus*	^{28}*leintwardinensis*	2
Clifton 13	0.708525 ± 0.000010	^{24}*progenitor*	^{25}*scanicus*	1
77-301	0.708543 ± 0.000012	^{24}*progenitor*	^{25}*scanicus*	1
M2-1	0.708457 ± 0.000011	^{23}*nilssoni*	^{23}*nilssoni*	None
77-24	0.708483 ± 0.000027	^{23}*nilssoni*	^{23}*nilssoni*	None
77-22	0.708440 ± 0.000009	^{22}*ludensis*	^{22}*ludensis*	None
Clifton 11	0.708426 ± 0.000011	^{21}*nassa*	^{21}*nassa*	None
Haragan Ck 9	0.708422 ± 0.000011	^{21}*nassa*	^{21}*nassa*	None
77-16	0.708468 ± 0.000012	^{20}*lundgreni*	^{23}*nilssoni*	3
77-20A	0.708343 ± 0.000010	^{18}*flexilis*	^{15}*murchisoni*	3
Centervile-9	0.708343 ± 0.000012	^{18}*flexilis*	^{15}*murchisoni*	3
Haragan Ck 4	0.708364 ± 0.000015	^{17}*regidus*	^{17}*regidus*	None
CA-103	0.708373 ± 0.000018	^{15}*murchisoni*	^{17}*regidus*	2
Haragan Ck 2	0.708343 ± 0.000011	^{15}*murchisoni*	^{15}*murchisoni*	None
77-12A	0.708371 ± 0.000020	^{14}*centrifugus*	^{16}*riccartonensis*	2
77-11	0.708328 ± 0.000008	^{14}*centrifugus*	^{14}*centrifugus*	None
Hughly Brook F	0.708362 ± 0.000012	^{14}*centrifugus*	^{16}*riccartonensis*	2
CA-102	0.708359 ± 0.000010	^{13}*crenulata*	^{13}*crenulata*	None
CA-101A	0.708357 ± 0.000010	^{13}*crenulata*	^{13}*crenulata*	None
Santa Fel 12656	0.708313 ± 0.000010	^{13}*crenulata*	^{13}*crenulata*	None
Love Hollow	0.708147 ± 0.000008	^{11}*crispus*	^{8}*convolutus*	3
267	0.708303 ± 0.000011	^{12}*grestonensis*	^{12}*grestonensis*	None
264	0.708261 ± 0.000011	^{12}*grestonensis*	^{12}*grestonensis*	None
260	0.708230 ± 0.000011	^{11}*crispus*	^{12}*grestonensis*	1
Gullet 2	0.708262 ± 0.000010	^{10}*turriculatus*	^{12}*grestonensis*	2
292	0.708242 ± 0.000010	^{10}*turriculatus*	^{12}*grestonensis*	2
281	0.708214 ± 0.000012	^{10}*turriculatus*	^{11}*crispus*	1
238	0.708166 ± 0.000009	^{8}*convolutus*	^{9}*sedgwekii*	1
Brassfield	0.708043 ± 0.000008	^{4}*cyphus*	^{4}*cyphus*	None
Pegasus 12005	0.707980 ± 0.000011	^{2}*avatus*	^{2}*avatus*	None
96573	0.707888 ± 0.000011	Ordovician-Silurian	Ordovician-Silurian	None
96567	0.707886 ± 0.000011	Ordovician-Silurian	Ordovician-Silurian	None
96557	0.707880 ± 0.000011	Ordovician-Silurian	Ordovician-Silurian	None

Notes: The $^{87}Sr/^{86}Sr$ values were normalized to the NBS 987 value of 0.710249. the superscript numbers, prior to biozones, refer to the same pattern of biozonation as in Figure 2. Duplicates, the outliers in the Landovery and the Přídolí samples were excluded from the test.

Correlation Based on Inflections

Points of inflection in the Sr-isotope curve can serve as reliable tie points that can be used for correlation (cf. McArthur, 1994), particularly when samples are taken at short intervals. Such trends can also be generated by postdepositional alteration, but excellent preservation of the sampled brachiopods appears to exclude the possibility of false signals. Stratigraphic hiatuses, when they do not include the inflection point, usually cause a shift in the position of inflections (McArthur, 1994), and correlation of such tie points may help to estimate the duration of the hiatus.

The Přídolían sections of Latvia (Kolka 54), Lithuania (Taurage 11), and Ukraine (Podolia) contain minor unconformities, yet their Sr-isotope curves all show three main inflections (Fig. 5) that correlate with the ^{36}*ultimus*, ^{38}*lochkovensis*, and ^{40}*permeri* biozones, respectively. The most significant inflection is the one in the ^{38}*lochkovensis* biozone, this biozone being characteristic of the Kaugatuma-Ohesaare stage boundary in the Baltic sections (Latvia and Lithuania) and of the Rashkov-Dzwingorod formation boundary in the Podolian section. This is in agreement with the lithostratigraphic record for the Podolian and Lithuanian sections (Fig. 1), but in the Latvian section (Kolka 54) the inflection is in the lower portion of the upper Kaugatuma stage (Fig. 6). Therefore, it is possible that the stratigraphic position of the Kaugatuma-Ohesaare boundary in the Latvian section may be shifted downward to a level of approximately the present K_3bL^1 / K_3bL^2 bed boundary (Figs. 5 and 6), but more work on stratigraphy and geochemistry is required to validate this proposition.

The Wenlockian Sr-isotope curves for Wales (United Kingdom), Gotland (Sweden), and Lithuania follow similar patterns (Fig. 7), with the $^{87}Sr/^{86}Sr$ inflection correlated with the ^{15}*murchisoni* biozone, where the decline that commenced in latest Telychian time (Fig. 2) is reversed. Samples from Gotland show a considerable drop in the $^{87}Sr/^{86}Sr$ record, also toward the *19ellesae* biozone, but in the other sections this was not confirmed due to lack of samples. The relatively large discrepancy in $^{87}Sr/^{86}Sr$ (~ 6 x 10^{-6}) in the *20lundgreni* biozone for the Lithuanian vs. United Kingdom and Gotland data needs to be resolved.

In conclusion, the use of inflection points in Sr-isotope stratigraphy is an effective technique for correlation of successions from different basins, particularly when sampling is done at close intervals in a high-resolution pattern.

Curve Testing

In order to test the reliability of the Sr isotope technique for correlation purposes, we have employed a set of $^{87}Sr/^{86}Sr$ values of Silurian conodonts from Ruppel et al. (1996), where the assignment of samples up to a biozone was known. The measured values were plotted onto the regressions in Figure 4, and on the basis of this projection, the samples were assigned to a specific graptolite biozone (Table 3). About 75% of the estimated correlations are within ±1 biozone and in many cases they agree completely. The results based on average curve in Figure 2 are in general comparable. This confirms the potential of Sr isotope stratigraphy as a correlation tool.

CONCLUSIONS

1. The progressive increase in the $^{87}Sr/^{86}Sr$ values of Silurian seawater with time (from 0.707930 to 0.708792) probably reflects an enhanced degree of weathering of the continental sialic rocks that may have been associated with warming of the climate during the Silurian.

2. The stepwise increase in $^{87}Sr/^{86}Sr$ values enables correlation with an accuracy of about ±2 biozones (~ 1.5 m.y.).

3. The Sr-isotope curve contains inflection points in the Wenlock and the Přídolí that may be utilized for correlation of sequences from United Kingdom, Gotland, Lithuania, Latvia, and Podolia.

ACKNOWLEDGMENTS

We thank D. Kaljo, P. Musteikis, and M. Rubel for providing and identifying samples, V. Gritsenko for assistance in the field, and B. Cousens for expert laboratory assistance. This project was financed by the Natural Sciences and Engineering Research Council of Canada, ESSO Resources Canada Limited (Imperial Oil), and Deutsch Forschuns-gemeinschaft.

REFERENCES CITED

Azmy, K., 1996, Isotopic composition of Silurian brachiopods: Implications for coeval seawater [Ph.D. dissert.]: Ottawa, Ontario, University of Ottawa, 197 p.

Azmy, K., Veizer, J., Bassett, M. G., and Copper, P., 1998, Oxygen and carbon isotopic composition of Silurian brachiopods: Implications for coeval seawater and glaciations: Geological Society of America Bulletin, v. 110, p. 1499–1512.

Banner, J. L., and Kaufman, J., 1994, The isotopic record of ocean chemistry and diagenesis preserved in nonluminescent brachiopods from Mississippian carbonate rocks, Illinois and Missouri: Geological Society of America Bulletin, v. 106, p. 1074–1082.

Bassett, M. G., Kaljo, D., and Teller, L., 1989, The Baltic region, *in* Holland, C. H., and Bassett, M. G., eds., A global standard for the Silurian System: Cardiff, National Museum of Wales, Geological Series no. 9, p. 158–170.

Bertram, C. J., Elderfield, H., Aldridge, R. J., and Morris, S. C., 1992, $^{87}Sr/^{86}Sr$, $^{143}Nd/^{144}Nd$ and REEs in Silurian phosphatic fossils: Earth and Planetary Science Letters, v. 113, p. 239–249.

Burke, W. H., Denison, R. E., Hetherington, E. A., Koepnick, R. B., Nelson, H. F., and Otto, J. B., 1982, Variation of seawater $^{87}Sr/^{86}Sr$ throughout Phanerozoic time: Geology, v. 10, p. 516–519.

Denison, R. E., Koepnick, R. B., Burke, W. H., Hetherington, E. A., and Fletcher, A., 1997, Construction of the Silurian and Devonian seawater $^{87}Sr/^{86}Sr$ curve: Chemical Geology, v. 140, p. 109–121.

Diener, A., Ebneth, S., Veizer, J., and Buhl, D., 1996, Strontium isotope stratigraphy of the Middle Devonian: Brachiopods and conodonts: Geochimica et Cosmochimica Acta, v. 60, p. 639–652.

Elderfield, H., 1986, Strontium isotope stratigraphy: Palaeogeography, Palaeoclimatology, Palaeoecology, v. 57, p. 71–90.

Farrell, J. W., Steven, C. C., and Gromet, L. P., 1995, Improved chronostratigraphic reference curve of late Neogene seawater $^{87}Sr/^{86}Sr$: Geology, v. 23, p. 403–406.

Faure, G., 1986, Principles of isotope geology (second edition): New York, John Wiley and Sons, 464 p.

Harland, W. B., Armstrong, R. L., Cox, A. V., Craig, L. E., Smith, A. G., and Smith, D. G., 1990, A geologic time scale: Cambridge, Cambridge University Press, 263 p.

Hodell, D. A., 1994, Progress and paradox in strontium isotope stratigraphy: Paleoceanography, v. 9, p. 395–398.

Hodell, D. A., and Woodruff, F., 1994, Variations in the strontium isotopic ratio of seawater during the Miocene: Stratigraphic and geochemical implications: Paleoceanography, v. 9, p. 405–426.

Hodell, D. A., Müller, P. A., McKenzie, J. A., and Mead, G. A., 1989, Strontium isotope stratigraphy and geochemistry of the late Neogene ocean: Earth and Planetary Science Letters, v. 92, p. 165–178.

Hodell, D. A., Mead, G. A., and Müller, P. A., 1990, Variation in the strontium isotopic composition of seawater (8 Ma to present): Implications for the chemical weathering rates and dissolved fluxes to the oceans: Chemical Geology, v. 80, p. 291–307.

Jin, J., Caldwell, W. G. E., and Copper, P., 1990, Evolution of the Early Silurian rhynchonellid brachiopod *Fenestrirostra* in the Anticosti Basin of Québec: Journal of Paleontology, v. 64, p. 214–222.

Kaminskas, D., and Musteikis, P., 1994, Quantitative evaluation of carbonate and terrigenous material influence on brachiopod distribution: Geologija, v. 17, p. 96–105.

Long, D. G. F., and Copper, P., 1994, The Late Ordovician–Early Silurian carbonate tract of Anticosti Island, Gulf of St. Lawrence, eastern Canada: Geological Association of Canada (GAC), Mineralogical Association of Canada (MAC), Joint Annual Meeting, Waterloo, Ontario, guidebook, Field trip B4: 69 p.

McArthur, J. M., 1994, Recent trends in strontium isotope stratigraphy: Terra Nova, v. 6, p. 331–358.

McKerrow, W. S., Dewey, J. F., and Scotese, C. R., 1991, The Ordovician and Silurian development of the Iapetus ocean: Special Papers in Palaeontology, v. 44, p. 165–178.

Mead, G. A., and Hodell, D. A., 1995, Controls on the $^{87}Sr/^{86}Sr$ composition of seawater from the middle Eocene to Oligocene: Hole 689B, Maud Rise, Antarctica: Paleoceanography, v. 10, p. 327–346.

Miller, K. G., Feigenson, M. D., Wright, J. D., and Clement, B. M., 1991, Miocene isotope reference section, Deep Sea Drilling Project Site 608: An evaluation of isotope and biostratigraphic resolution: Paleoceanography, v. 6, p. 33–52.

Montañez, I. P., Banner, J. L., Osleger, D. A., Borg, L. E., and Bosserman, P. J., 1996, Integrated Sr isotope stratigraphy and relative sea-level history in Middle Cambrian platform carbonates: Geology, v. 24, p. 917–920.

Neuman, B. E. E., and Kershaw, S., 1991, VI International symposium on Fossil Cnidaria including Archaeocyatha and Porifera, *in* Excursion guidebook, Pro symposium excursion A1 Gotland/Sweden Silurian reefs and coral-bearing strata: Bergen, 111 p.

Oslick, J. S. Miller, K. G., and Feigenson, M. D., 1994, Oligocene-Miocene strontium isotopes: Stratigraphic revisions and correlation to an inferred glacioeustatic record: Paleoceanography, v. 9, p. 427–443.

Palmer, M. R., and Elderfield, H., 1985, Sr isotope composition of seawater over the past 75 Myr: Nature, v. 314, p. 526–528.

Popp, B. N., Anderson, T. F., and Sandberg, P. A., 1986, Brachiopods as indicators of original isotopic compositions in some Paleozoic limestones: Geological Society of America Bulletin, v. 97, p. 11262–1269.

Quinn, T. M., Lohmann, K. C., and Halliday, A. N., 1991, Sr isotopic variation in shallow water carbonate sequences: Stratigraphic, chronostratigraphic, and eustatic implications of the record at Enewetak Atoll: Paleoceanography, v. 6, p. 371–385.

Richter, F. M., Rowley, B. D., and DePaolo, D. J., 1992, Sr isotope evolution of seawater: The role of tectonics: Earth and Planetary Science Letters, v. 109, p. 11–23.

Ruppel, S. C., James, E. W., Barrick, J. E., Nowlan, G., and Uyeno, T. T., 1996, High-resolution $^{87}Sr/^{86}Sr$ chemostratigraphy of the Silurian: Implications for event correlation and strontium flux: Geology, v. 24, p. 831–834.

Siveter, D. J., Owens, R. M., and Thomas, A. T., 1989, The northern Wenlock Edge area: Shelf muds and carbonates on the Midland Platform, *in* Bassett, M. G., ed., Silurian field excursions, A geotraverse across Wales and the Welsh Borderland: Cardiff, National Museum of Wales, Geological Series no. 10, p. 23–35.

Veizer, J., 1989, Strontium isotopes in seawater through time: Annual Reviews of Earth and Planetary Science, v. 17, p. 141–167.

Veizer, J., and Compston, W., 1974, $^{87}Sr/^{86}Sr$ in Precambrian carbonates as an index of crustal evolution: Geochimica et Cosmochimica Acta, v. 40, p. 905–915.

Wenzel, B., 1997, Isotopenstratigraphische Untersuchungen an silurischen Abfolgen und deren paläozeanographische Interpretation: Erlanger Geologische Abhandlungen, v. 129, p. 1–117.

Wenzel, B., and Joachimski, M. M., 1996, Carbon and oxygen isotopic composition of Silurian brachiopods (Gotland/Sweden)— Palaeoceanographic implications: Palaeogeography, Palaeoclimatology, Palaeoecology, v. 122, p. 143–166.

MANUSCRIPT RECEIVED BY THE SOCIETY APRIL 28, 1997
REVISED MANUSCRIPT RECEIVED APRIL 2, 1998
MANUSCRIPT ACCEPTED APRIL 21, 1998

Printed in U.S.A.